



Dimensions of continents and oceans – water has carved a perfect cistern



J.A. Whitehead

Department of Physical Oceanography, Woods Hole Oceanographic Institution, Woods Hole, MA 02540, USA

ARTICLE INFO

Article history:

Received 26 August 2016

Received in revised form 17 December 2016

Accepted 11 March 2017

Available online 30 March 2017

Editor: C. Sotin

Keywords:

freeboard

continental crust depth

ocean depth

continent area

ocean area

continental crust and water volumes

ABSTRACT

The ocean basins have almost exactly the correct surface area and average depth to hold Earth's water. This study asserts that three processes are responsible for this. First, the crust is thickened by lateral compression from mountain formation. Second, Earth's continental crust is leveled by erosion. Third, due to the efficiency of erosion, the average elevation is a few hundred meters above sea level. A theoretical fluid model, suggested partly by laboratory experiments, includes an ocean of specified depth. The resulting continents are tabular (that is, their elevation view is rectangular). The surface lies above sea level, contributing to a well-known double maximum in Earth's elevation corresponding to continents and ocean basins. Next, a simple hydrostatic balance between continent and ocean gives average depth and area of present oceans and continents within 33%. Further calculations with a suitable correction to fit present Earth cover a wide range of possible crust volumes for earlier Earth. With the present water volume, ocean area always exceeds 25% of the globe. For all possible water volumes, average continental crust thickness always exceeds 23.4 km. This may explain why cratons have thicknesses comparable to younger crust so that they are found on Earth's surface today. Therefore, mountain building and erosion have enabled water to carve its own cistern in the form of the accumulated ocean basins. The wide range of areas and depths of oceans and continents found here can constrain models of early earth. Similar calculations can be done for earthlike planets as well.

© 2017 Elsevier B.V. All rights reserved.

1. Introduction

It is well known that Earth's ocean basins average approximately 3800 m (2.5 miles) depth covering approximately 70% of the surface and containing 97% of the world's water (e.g. Sverdrup et al., 1942). The deep ocean basins contain even closer to 100% of Earth's liquid water during glacial periods. Therefore, continents and oceans have come to a balance so that the ocean basins hold almost all of the water. This balance possibly has some effect on planetary climate, although there is at least one suggestion that this might only apply to second order (Kuhn et al., 1989).

Geochemists know that orogeny, volcanism, and sedimentation, contribute to the chemical evolution and building of continental material (e.g. Dewey and Windley, 1981; McLennan and Taylor, 1983; Cogley, 1984; Taylor and McLennan, 1995; Saal et al., 1998; Clift and Vannuchi, 2004; Hawkesworth et al., 2010; Walther, 2005; O'Neill et al., 2015). The mechanical consequences of orogeny, volcanism and sedimentation seem to be studied less. How did the continents and ocean basins mechanically evolve so that the oceans have exactly the correct area and average

depth to hold Earth's water? Did the overall dimensions of continents and oceans have their origin in the balances between mountain building and erosion rate (Harrison, 1994; Zhang, 2005; Roberts et al., 2015)? Here, the freeboard concept (Wise, 1972, 1974) is added as in Whitehead and Clift (2009), which leads to mean continent elevation being only a few hundred meters above sea level.

Mountain building is a direct consequence of the great rigid "tectonic" plates moving over Earth's surface. It is well known that the ocean floor on each plate is produced and moves away from mid-ocean ridges at divergent margins, and the floor is consumed by sinking (subducting) into the interior of the earth (the mantle) in subduction zones at convergent margins. Therefore, any fixed thing within a plate, including a continent, migrates from divergent to convergent margins. Once a continent arrives at a subduction zone, compression and orogeny occurs and mountain belts are produced (Press, 2003; Johnson and Harley, 2012). Over 80 orogenic events exist in the geological record over roughly four billion years (Kearey et al., 2009; Johnson and Harley, 2012) pointing to the possibility of plate tectonics existing over that period of time. Although each event has a special story (e.g. Royden, 1993a; Kaufman and Royden, 1994; Huerta et al., 1996, 1998, 1999;

E-mail address: jwhitehead@whoi.edu.

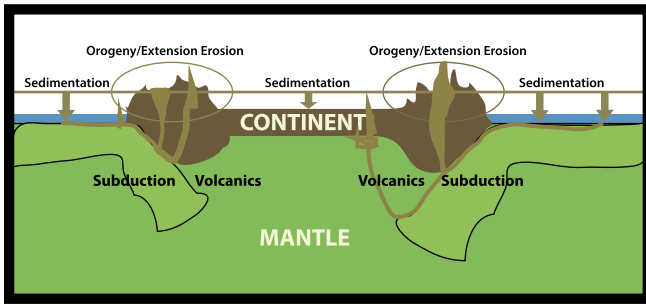


Fig. 1. Processes altering the thickness and areas of continents and oceans to first order.

Thatcher et al., 1999; Yin and Harrison, 2000), during each event, the continental crust is thickened. Orogeny produces a thickness increase of 2.5% in the past 65 my (Clift and Vannuchi, 2004; Whitehead and Clift, 2009). The thickening decreases the total continent area by 1.7% and consequentially increases ocean area.

This persistent crustal thickening is balanced to first order by redistribution of continental material by erosion (Harrison, 1994). The erosion rates are sufficiently great to erode the continent surface down to an elevation close to sea level. Estimates of time scales for erosion of mountain belts are a few hundred million years (Veizer and Jansen, 1985; Harrison, 1994; Zhang, 2005; Clift et al., 2009). The average surface elevation is presently only 835 m above sea level, so earth has tabular continents that lead to the well-known double maximum in elevation distribution (Sverdrup et al., 1942; Harrison, 1988, 1990, 1998; Harrison et al., 1981, 1983, 1985). This distribution is not observed for other rocky planets and moons (Uchupi and Emery, 1993).

The eroded continental material deposited on the seafloor is ultimately buried at subduction zones (Clift et al., 2009). This material feeds volcanism that produces new continent material through andesitic lavas at continent margins (Gazel et al., 2015). The cycle of water into and out of the mantle is also involved in generating new continental crust (Höning and Spohn, 2016). Another contributor to continent area increase is internal deformation, which is best documented as strongly localized divergence within mountainous regions (Kaufman and Royden, 1994; Huerta et al., 1996, 1998, 1999; Royden, 1993b; Thatcher et al., 1999; Bird, 1979; Kay and Kay, 1993; Conrad and Molnar, 1997; Houseman and Molnar, 1997). For example, calculations based on measurements of Himalayan spreading and uplift have produced estimates of the viscosity of the continental material (England and Molnar, 1997; Flesch et al., 2000). There is no present estimate of continent divergence globally.

Finally, the freeboard effect notes that continent edges are almost exactly at sea level as a consequence of erosion, which is more effective under air than under the ocean surface (Wise, 1972, 1974; Harrison, 1998, 1999; Eriksson, 1999; Hynes, 2001; McElroy and Wilkinson, 2005). This effect, plus the strength of erosion (Wise, 1972, 1974; Harrison, 1998, 1999; Hynes, 2001; McElroy and Wilkinson, 2005) limits the average elevation of the continents to under 1 km above the sea surface.

The balance between mountain building; continent extension; erosion; sedimentation; the burial of sediments in the mantle; and the eventual return of some of the sediment material and water to the continents is summarized in Fig. 1. The purpose of this paper is to present a simple fluid mechanical model of this and to report some consequences of ensuing calculations. In Section 2, some fluid experiments show how thickening of a floating fluid from convergence of an underlying fluid leads to elevation of the surface. In Section 3, a fluid theory produces the tabular nature of continents when the floating fluid is in the presence of an ocean. In Section 4, a simple calculation explores a ba-

sic consequence of the constraint that continent elevation has a fixed value above sea level. This simple isostatic calculation quantifies one of the fundamental features of earth and oceans, yet it appears to be absent from textbooks and summarizing articles about Earth (e.g. Schubert and Sandwell, 1989; Turcotte and Schubert, 2002; Press, 2003; Grotzinger and Jordan, 2010; King, 2015; Condie, 2016). Then, additional calculations use other possible volumes of crust and water for an earlier Earth constraint.

2. Suggestive laboratory experiments

Laboratory experiments were constructed to quantify the balance of crustal thickening and spreading. The first experiment has a layer of high viscosity silicon oil floating above corn syrup in a rectangular container (Fig. 2). The roller on the right rotates counterclockwise, and the one on the left rotates clockwise at the same rate. Convergence at the oil–syrup interface driven by the two rollers thickens the center of the layer of floating oil and elevates the surface (Fig. 2b). For sufficient roller speed, the oil separates from the walls (Fig. 2c). Vertical thickening along the center of the tank increases with roller speed (Fig. 3). This agrees with a linear theory developed in the Appendix. Using densities and viscosities of the laboratory materials, the maximum elevation of the top surface e (see the table in supplementary material for a list of symbols), as a function of roller angular rotation rate Ω , is given by the formula $e = 1.36 \times 10^{-3} \Omega$ and the depression of the interface d_{in} is given by $d_{in} = 3.31 \times 10^{-3} \Omega$. Therefore, elevation is proportional to driving rate Ω .

The second experiment shows that the elevated surface is not dependent on Newtonian viscosity. It has a top layer of 600 polypropylene balls of 0.64 cm diameter combined with 100 balls of 0.32 cm diameter floating in silicon oil with kinematic viscosity $10 \text{ cm}^2 \text{ s}^{-1}$ lying under air. The combination of sizes of balls produces a mushy matrix. They occupy half of the interior volume of a transparent circular cylinder whose rotational axis is tangential to gravity. A circulation cell in the oil is driven by steady slow counterclockwise rotation, sweeping the floating balls toward the descending region on the left (Fig. 4). There, the balls collect in a deep patch. The surface of the balls in the patch lies above the level of the fluid, even though they are located above the descending oil.

All experiments show that the top surface of the thickened patch extends upward. The elevation of the top layer in Fig. 3 depends on the speed of the driving, so this experiment does not include the two different rates of erosion under air and under water that are vital to Wise's explanation of freeboard. Therefore, a simplified model and its theory is developed that will incorporate the two different rates of flattening for continent surfaces below and above water consistent with the freeboard concept.

3. A mechanical model of a continent with the ocean present

This model has floating viscous fluid that is thickened by convergence from a velocity imposed at the base of the continent material. To incorporate gravitational spreading that balances this convergence, we take note of a popular parameterization for erosion that flattens the continent surface in accordance with the relation

$$\frac{\partial h}{\partial t} = -Kh. \quad (1)$$

Typically, the erosion rate K is proportional to an erosion coefficient determined by the land size, and inversely proportional to an erosion boundary layer depth and an isostatic factor (e.g. Zhang, 2005). In addition, K typically is a nonlinear function of slope. However, for simplicity our model makes K a constant and we assign a viscosity to the continent material, making it a Newtonian fluid.

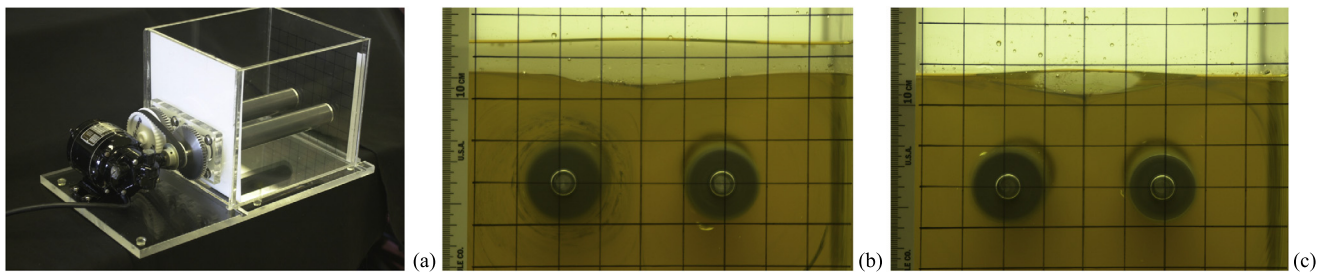


Fig. 2. (a) The experimental apparatus with a flow driven by 2 rollers. This produces two overturning cells in the bottom fluid that exert stress to the upper fluid. (b) The top layer thickens at the center with upward deflection of the center for slow roller speed. (c) At higher roller speed, the surface layer is swept into an isolated body.

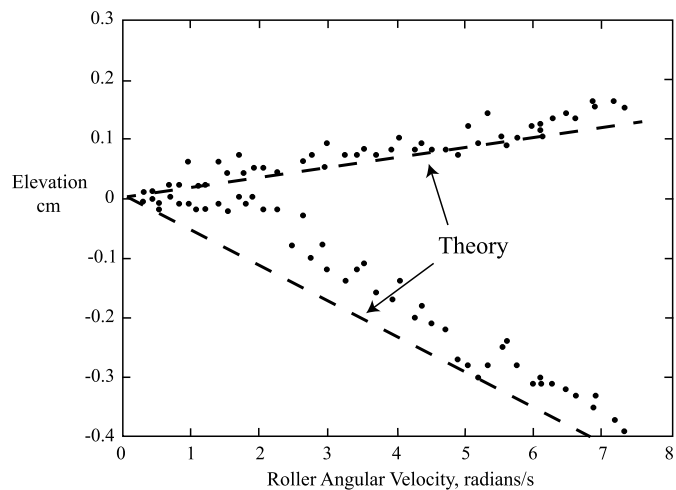


Fig. 3. Elevation of the top and depression of the interface as a function of roller rotation rate Ω . The dashed lines are from equations (A.10) and (A.11).

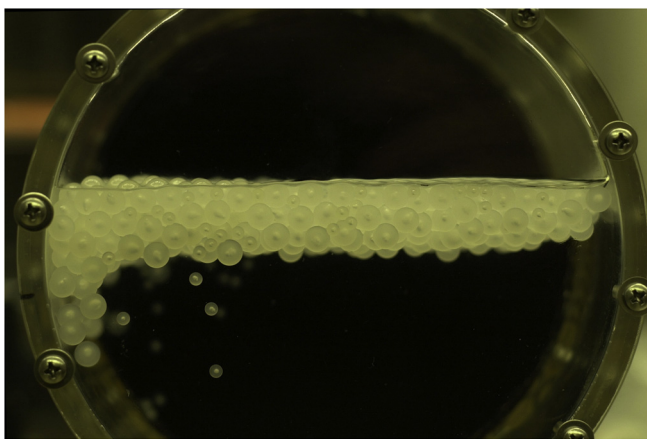


Fig. 4. Photograph of a cluster of floating spheres in a counterclockwise slowly rotating cylinder 13.3 cm in diameter half full of silicon oil. The camera looks along both the axis of the cylinder and along the rotation axis. Gravity is directed downward.

Our model is a simplification of the dynamics of the continental crust (Fig. 5a). Flow at the base of the crust imposed by mantle flow pushes the deep continental material toward the right (Fig. 5a, b). The surface tilts upward toward the right to provide a hydrostatic pressure gradient to drive the return flow. This is the exact balance discussed by Zhang (2005), who parameterized erosion more fully than is to be done here. Although earth has more than one continent, this model represents an average of all the continents.

In the mathematical model (Fig. 5b), three fluids representing ocean, continent and mantle have densities ρ_o , ρ_c , and ρ_m . They

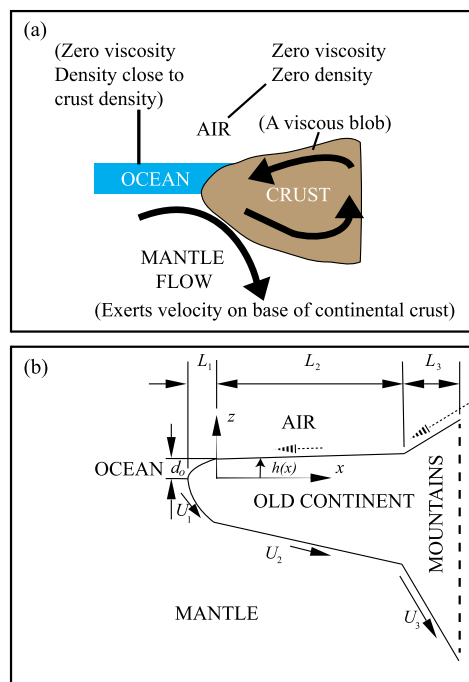


Fig. 5. Elevation views of the simplified equilibrium state of the continents and oceans. Vertical direction is stretched greatly. (a) A cartoon of the dynamics. Surface flow corresponding to erosion is generated by viscous flow within the continent, driven by bottom velocity. (b) Geometry of the theory. The surface flow shown by dashed arrows represents downhill movement of the surface through erosion.

all lie in a field of gravity with acceleration g downward. Air lies over everything but it has negligible density and viscosity. The ocean has depth d_0 , and the continent has kinematic viscosity ν . The continent has three regions: 1. The first is an old continent region under the surface. 2. This is an old continent region lying under air. 3. Finally there is a region of mountains.

In all three regions, motion is imposed at the base of the continent by specifying velocities. Regions 1 and 2 are characterized by different surface restoring forces as models of erosion under water and under air, and they have a constant positive normal speed $U_1 = U_2$. Region 3 has a greater normal speed U_3 . This faster flow rate under mountains represents convergence of the mantle in subduction zones that produce mountain belts. The return flows are shown in Fig. 5b by dashed arrows. Return flows are meant to represent and to simulate erosion and not actual creep of the continent material. Slope is largest in Region 1 from a smaller restoring force that represents small erosion rate. Regions 2 and 3 are characterized with two different bottom speeds. Therefore, the mountains have a greater return flow in a negative direction than the return flow of old continent under air. This is represented by the dashed arrow under L_3 . Surface slope is smallest in Region 2.

The continent thickness and surface slope are calculated as a function of the ocean depth, velocities, and physical properties of the materials. It will be assumed that the aspect ratio d_0/L_2 is small. Although the speeds are free to vary over wide ranges of possible relevance to Earth, Stokes flow is anticipated. This limit is defined using the speed under region 2 as a typical speed so that $U_2 d_0/\nu \ll 1$. To model the weak erosion rate of the continent surface under water compared to erosion rate of the continent surface under the atmosphere, we specify $\rho_2 - \rho_1 \ll \rho_2$. In other words, this model uses a small surface restoring force to represent small erosion under the ocean. Thus, the density of ordinary water is not used but instead a density close to continent density is given for the ocean. This small density difference is an artifice to insure that the surface restoring force of the continent under water is much less than the surface restoring force to the continent under air.

In this model, the flow within the continent is the only unknown flow. The continent fluid obeys continuity and Stokes flow.

$$\nabla \cdot \tilde{u}_i = 0 \quad (2)$$

$$\nabla p_i = \mu \nabla^2 \tilde{u}_i - g \rho_c \hat{k} \quad (3)$$

with \tilde{u}_i the velocity vector and p_i the pressure. The ocean and atmosphere are low in viscosity compared to the continent, producing negligible stresses on the continent except for hydrostatics. In addition, atmospheric pressure is zero at sea level and along the continent surface. Third, the flow is strictly two dimensional in the vertical and lateral plane.

The vertical origin is located at the ocean floor (Fig. 5), and the lateral origin is located at the continent–sea surface point of intersection. Taking the limit $d_0^2/L_2^2 \ll 1$ (with L_2 a typical lateral length), the common lubrication approximation exists with negligible vertical velocities and lateral derivatives. The hydrostatic equation governs vertical forces for the continents.

We first develop the equations in the regions under air (Regions 2 and 3). The pressure obeys $p_i = 0$ at $z = h_i(x)$ ($i = 2, 3$), where h_i is the surface elevation above the ocean floor. The hydrostatic approximation is

$$p_i = g \rho_c (h_i - z). \quad (4)$$

Therefore, the lubrication approximation is valid in the lateral direction, and since it has only vertical derivatives, the equation in each region is

$$\frac{1}{\rho_c} \frac{\partial p_i}{\partial x} = g \frac{\partial h_i}{\partial x} = \nu \frac{\partial^2 u_i}{\partial z^2} \quad (5)$$

with solution

$$u_i = \frac{g}{\nu} \frac{\partial h_i}{\partial x} \frac{z^2}{2} + A_i z + B_i. \quad (6)$$

This approach resembles simple lubrication theory as applied for example for asthenospheric flow and return flow (Turcotte and Schubert, 2002). The depth of the base of the continent is determined by setting pressure below it to the hydrostatic value using the hydrostatic approximation,

$$z = \delta h_i(x) \quad (7)$$

where $\delta = \rho_c / (\rho_m - \rho_c)$. We set $u_i = U_i$ there to get

$$B_i = U_i - \frac{g}{\nu} \frac{\partial h_i}{\partial x} \frac{z^2}{2} + A_i \delta h_i. \quad (8)$$

In addition, the lateral shear at the continent surface is set to zero giving

$$A_i = -\frac{g}{\nu} \frac{\partial h_i}{\partial x} h_i. \quad (9)$$

Inserting these in (6),

$$u_i = \frac{g}{\nu} \frac{\partial h_i}{\partial x} \left(\frac{1}{2} (z^2 - \delta^2 h_i^2) - h_i (z + \delta h_i) \right) + U_i. \quad (10)$$

Lateral volume flux F_i is

$$F_i = \int_{-\delta h_i}^{h_i} u_i dz = -\frac{1}{3} \frac{g}{\nu} \frac{\partial h_i}{\partial x} (1 + \delta)^3 h_i^3 + U_i (1 + \delta) h_i. \quad (11)$$

Steady state

For a continent that is steady and fully developed, $F_i = 0$ so that

$$\frac{\partial h_i}{\partial x} = \frac{3\nu U_i}{g h_i^2 (1 + \delta)^2}. \quad (12)$$

This integrates to

$$h_i^3 = \frac{9\nu U_i x}{g(1 + \delta)^2} + C_i. \quad (13)$$

In region 2, $h = 0$ at $x = 0$ so $C_2 = d_0^3$ and the elevation is

$$h_2^3 = d_0^3 + \frac{9\nu U_2 x}{g(1 + \delta)^2}. \quad (14)$$

In region 3, the integration starts from the point where the surfaces are matched at $x = L_2$ so the elevation is

$$h_3^3 = d_0^3 + \frac{9\nu U_3 x}{g(1 + \delta)^2} + \frac{(U_2 - U_3)\nu L_2}{g(1 + \delta)^2}. \quad (15)$$

Now we consider region 1 under water. To calculate the surface, we use (13) with g replaced by reduced gravity $g' = g(\rho_c - \rho_o)/\rho_c$ so that

$$h_1^3 = d_0^3 + \frac{9\nu U_1 x}{g'(1 + \delta)^2}. \quad (16)$$

The lateral length for region 1 is found setting $h = 0$, at $x = -L_1$ so

$$L_1 = \frac{g'(1 + \delta)^2 d_0^3}{9U_1 \nu}. \quad (17)$$

Since we specify $g' \ll g$, for the purpose of determining a volume of the crust in this region, we approximate $L_1 = 0$.

For use in the following section, it is necessary to find the volume of the continent. Assuming that this 2 dimensional model has a typical width w in the third direction, and noting that the total depth of the continent at each point is given by $(1 + \delta)h_i(x)$, the volume of each region is

$$V_1 = 0 \quad (18)$$

$$\begin{aligned} V_2 &= w \int_0^{L_2} (1 + \delta) \left(d_0^3 + \frac{9U_2 \nu x}{g} \right)^{1/3} dx \\ &= \frac{3}{4} w (1 + \delta) \left(\frac{9U_2 \nu}{g} \right)^{1/3} \\ &\quad \times \left\{ \left(L_2 + \frac{g d_0^3}{9U_1 \nu} \right)^{4/3} - \left(\frac{g d_0^3}{9U_1 \nu} \right)^{4/3} \right\} \end{aligned} \quad (19)$$

$$\begin{aligned} V_3 &= \frac{3}{4} w (1 + \delta) \left(\frac{9U_3 \nu}{g} \right)^{1/3} \\ &\quad \times \left\{ \left(L_2 + L_3 + \frac{g(1 + \delta)^2 d_0^3}{9U_3 \nu} + \frac{(U_2 - U_3)L_2}{9U_3} \right)^{4/3} \right. \\ &\quad \left. - \left(L_2 + \frac{g(1 + \delta)^2 d_0^3}{9U_3 \nu} + \frac{(U_2 - U_3)L_2}{9U_3} \right)^{4/3} \right\} \end{aligned} \quad (20)$$

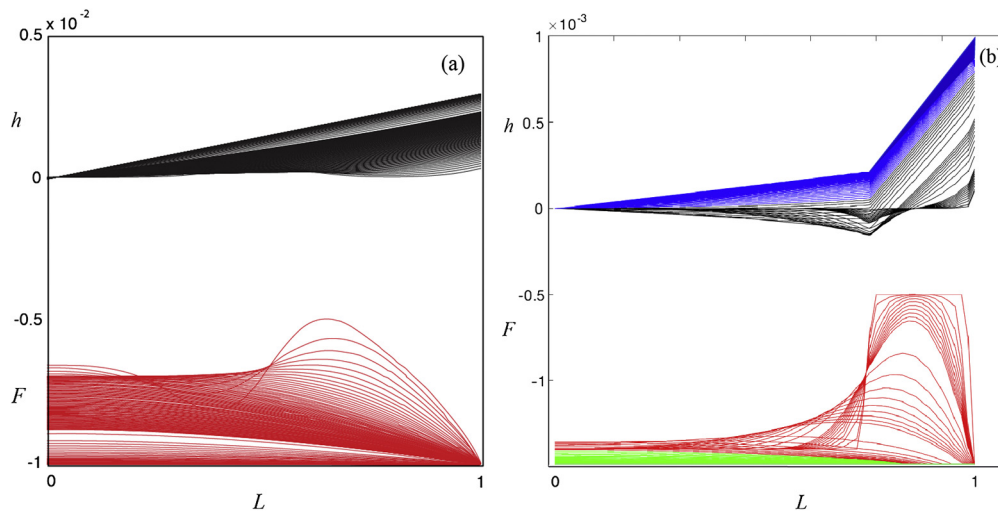


Fig. 6. Transient response of surface elevation and flux driven by a moving bottom. (a) Uniform speed $U_2\nu/gd_0^2 = 10^{-5}$. A bump that is initially placed in the middle relaxes with time. Elevation values are multiplied by five to show details. Time is normalized by dividing by timescale ν/gd_0 . Time intervals are 0.1 units. A value of 10^{-3} is subtracted from flux to offset it from zero. (b) There are different driving speeds in two regions. On the right, the speed is ten times greater. Time intervals are 0.01 units before $t = 0.1$, then intervals are 0.1 up to $t = 1$, then intervals are 1 (blue/green) up to $t = 4$. Flux F is normalized by dividing by gd_0^3/ν and a value of 0.15×10^{-3} is subtracted to offset it from zero. (For interpretation of the references to color in this figure legend, the reader is referred to the web version of this article.)

It is convenient to approximate these volumes.

$$V_1 = 0. \quad (21)$$

In regions 2 and 3, the elevation is expanded as a Taylor series about the left hand point that starts each region so that

$$V_2 = wd_0(1 + \delta)L_2 \left\{ 1 + \frac{\nu U_2 L_2}{6g(1 + \delta)^2 d_0^3} \right\} \quad (22)$$

$$V_3 = wd_0(1 + \delta)L_3 \left(1 + \frac{\nu U_2 L_2}{3g(1 + \delta)^2 d_0^3} \right) \left(1 + \frac{\nu U_3 L_3}{3g(1 + \delta)^2 d_0^3} \right) \quad (23)$$

To make realistic tabular continents, the term on the right within the brackets in (22) must be small so that the old continent has roughly constant thickness. This is true if $\frac{\nu U_2 L_2}{6g(1 + \delta)^2 d_0^3} < 1$. Using present Earth values in mks units of $g = 10 \text{ m s}^{-2}$, $d_0 = 3800 \text{ m}$, $\rho_2 = 2800 \text{ kg m}^{-3}$, $\rho_3 = 3300 \text{ kg m}^{-3}$, and $L_2 = 10^7 \text{ m}$, this requires that $\nu U_2 < 2.5 \times 10^3$. If one uses a speed associated with 0.1 times a value for mantle convection of $0.3 \times 10^{-9} \text{ m s}^{-1}$ the continent kinematic viscosity in this model has to be significantly smaller than $22.5 \times 10^{12} \text{ m}^2 \text{ s}^{-1}$. This is a value lower than commonly used mantle viscosity values that are approximately $10^{17} \text{ m}^2 \text{ s}^{-1}$ (Turcotte and Schubert, 2002), but such a small value is appropriate here since it quantifies the effects of erosion. It is similar in magnitude to values of erosion by Zhang (2005) with timescales of 10^8 yr , and who used an empirical value for uplift rate of similar magnitude that fits the present continents. The smallness of this viscosity compared to mantle viscosity gives a measure of the strength of erosion needed for Earth to have tabular continents (also discussed by Zhang, 2005). This low value suggests that the early experiments in Section 2 and the theory in Appendix A might be revisited using lower continent viscosity. However, a layer corresponding to the ocean should also be added. In region 3, one would specify a lateral length perhaps $L_3 = 10^6 \text{ m}$ with bottom speed 20 times greater.

The important result for this model of the continent is that the body is not tabular because of its strength, but because the rate of erosion flattening the continent is greater than the rate of mountain generation. This result is also pointed out by Zhang (2005). However, we also have added the fact that the ocean imposes a freeboard constraint. Although it can be argued that the freeboard–

orogeny–erosion balance applies to earth, supporting this through analysis from data about orogeny in addition to the rates of erosion already quantified by Zhang (2005) is beyond the scope of this paper.

Transient adjustment

The surface evolution is driven by conservation of volume flux

$$(1 + \delta) \frac{\partial h_i}{\partial t} = \frac{\partial F_i}{\partial x}, \quad (24)$$

which can be advanced numerically. The timescale is ν/gd_0^2 , the speed scale is $U_2\nu/gd_0^2$ and the dimensionless area flux scale is gd_0^3/ν . Fig. 6 shows a calculation in which there is only one region corresponding to Region 2 with no Region 3. The surface h gradually approaches a slope with a value of 3×10^{-5} . Note that an initial bump is substantially smoothed out after one time unit.

4. Areas and thicknesses of ocean and continent

In section 2, the experiments essentially had no ocean at all, so $d_0 = 0$. In section 3, the ocean depth d_0 is specified. Here, the value of d_0 is determined using simple hydrostatic equations. In the previous section, the pressure under the ocean was not a factor in the model. The pressure under the continents was hydrostatic and consistent with lubrication theory. In this section, the ocean lies over Earth's mantle and contributes to pressure in the mantle. The mantle, continent and ocean are not moving and a hydrostatic balance exists between ocean and continent. The cartoon in Fig. 7a (taken from Fig. 1) shows the factors contributing to the thickness of the continent. The cartoon in Fig. 7b shows the hydrostatic model analyzed here. The continents are aggregated together as one solid body that is floating on a liquid mantle. It lies next to a motionless liquid ocean.

Pressures within the mantle under ocean and continent are calculated using hydrostatics and set equal to each other. Mantle pressure under the oceans equals the weight per unit area from the accumulation of ocean water of depth d_o and mantle of thickness d_m . This is set equal to the weight per unit area under the continents of thickness d_c due to the continental crust. Hydrostatic pressure is calculated using the densities of ocean ($\rho_o = 1030 \text{ kg m}^{-3}$), continent ($\rho_c = 2800 \text{ kg m}^{-3}$), and mantle

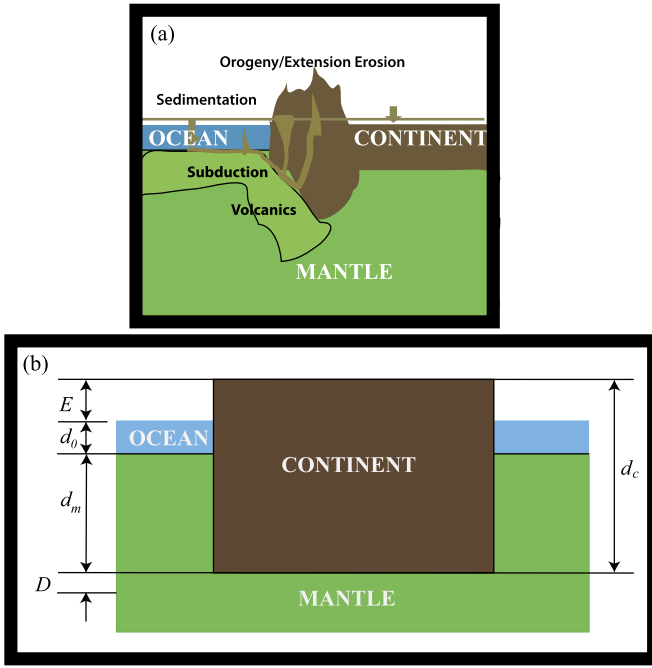


Fig. 7. (a) Sketch of the first-order factors modifying the thickness of the continental crust. (b) The hydrostatic balance of ocean basins and continents. (Simplified from Fig. 5 in Whitehead and Clift, 2009.)

($\rho_m = 3300 \text{ kg m}^{-3}$). The equality of pressure under ocean and continent obeys the formula

$$2800gd_c = 1030gd_o + 3300gd_m + 3300gD \quad (25)$$

with g the acceleration of gravity. The constant D is added to the equation to correct for everything left out of this model. The list of possible causes of corrections is long and includes many layers in the ocean floor, within the continents and in the upper mantle as well as features of mantle convection and even the density of air.

Defining E as the elevation of the continent above sea level, and using the relation $E + d_o + d_m = d_c$ to eliminate d_m from (25),

$$E = \frac{3300 - 2800}{3300}d_c - \frac{3300 - 1030}{3300}d_o + D. \quad (26)$$

Next, the known values of the volumes of continental crust and water are incorporated. Using volume V , area A and the subscript o for ocean, and c for continent, where

$$d_c = V_c/A_c \quad (27)$$

and

$$d_o = V_o/A_o. \quad (28)$$

Using the fact that the two areas add up to the surface area of Earth

$$A_o + A_c = 510 \times 10^6 \text{ km}^2 \quad (29)$$

A_o is eliminated using (28) and (29) and (26) becomes

$$E = \frac{500}{3300}d_c - \frac{2270V_o d_c}{3300(5.1 \times 10^8 d_c - V_c)}. \quad (30)$$

This reduces to the quadratic equation for crust thickness

$$2.55 \times 10^{11} d_c^2 - (500V_c + 2270V_o - 1.683 \times 10^{12}(D - E))d_c - 3300V_c(D - E) = 0 \quad (31)$$

with solution

$$d_c = F \pm \sqrt{F^2 + 1.294 \times 10^{-8} V_c (D - E)} \quad (32)$$

where $F = (500V_c + 2270V_o - 1.683 \times 10^{12}(D - E))/5.10 \times 10^{11}$.

Does (32) produce a reasonable prediction of depth of continental crust on Earth as a function of water and crust volumes? First, we ignore all deviations between this model and Earth by setting $D = 0$ and using the values $V_c = 7.679 \times 10^9 \text{ km}^3$ and $V_o = 1.178 \times 10^9$ (Whitehead and Clift, 2009). Using the present value of continent elevation above the sea surface $E = 0.835 \text{ km}$ (Turcotte and Schubert, 2002) in equation (32), we get $d_c = 28.1 \text{ km}$. This depth is 73% of the present average crust thickness $d_c = 38.4 \text{ km}$ (Whitehead and Clift, 2009). Continent area using this thickness and the present volume of crust is $2.67 \times 10^8 \text{ km}^2$, which is 133% of the actual area of $2 \times 10^8 \text{ km}^2$. Consequent ocean area is $2.53 \times 10^8 \text{ km}^2$, which is 81% of the actual area of $3.10 \times 10^8 \text{ km}^2$. The fact that all these values are within 34% of earth's values indicates that this extremely crude model is a good first approximation.

It is clear that secular changes in the value of D might arise, for example from secular changes in heat flow (Schubert and Reyrer, 1985). It is not the object here to determine a better value of the present value of D from direct geophysical measurements (e.g. Gossler and Kind, 1996), although that would make a useful future study. Instead, we use the present crust thickness $d_c = 38.4 \text{ km}$ to calculate the value of D for present Earth and it is $D = -2.369 \text{ km}$. Naturally, using (26) with this value of D gives the present value of ocean depth $d_o = 3.8 \text{ km}$ (Whitehead and Clift, 2009) as well as the correct ocean and continent areas.

It is useful to insert $D = -2.369 \text{ km}$ in (32) and find possible thicknesses and areas for earlier earth by considering plausible ranges of volumes of early continental crust and water. Here Earth's present area is used. In addition, since early erosion is not easily quantified, a number of values of E (Müller et al., 2008) are considered. Fig. 8a shows the continental crust thickness as a function of V_c for assorted values of E using the present day value of D and the present ocean volume (a value consistent with the present ocean area $A_o = 310 \times 10^6 \text{ km}^2$, and ocean depth $d_o = 3.8$ (Whitehead and Clift, 2009). Values of ocean depth (Fig. 8b) can also be found since it is linearly related to crust thickness by (26). The curves are the same as those in Fig. 8a but with different offset.

Fig. 8 shows a number of things: First, d_c extends from approximately 25 to 66 km in thickness. Second, the spread of the curves for different values of E means that continent thickness is sensitive in detail to continent elevation and hence, presumably to erosion rate. Third, since E and D are subtracted in equation (32), thickness is also sensitive to the exact value of D . Therefore, if early continent or mantle structures differ significantly from their present structures, the effect would be similar to the effects of different levels of erosion. Fourth, ocean depth varies considerably because d_o ranges from just over 2 km up to almost 11 km. Since (26) shows that d_o is linearly proportional to d_c , the curves in (a) and (b) have the same shape even though relative offsets are different. Fifth, and most importantly, even with this wide range of E (hence D), continental crust thickness never is less than 25 km. The result that crustal thickness exceeds a certain value is consistent with the fact that the crust of cratons has thicknesses of the order of present crust (King, 2005), resulting in cratons covering a significant part of the present continents (Fig. 9).

The crust thickness d_c is related to areas of continent and ocean in (27)–(29). Fig. 10 shows results for the same parameters as used to make Fig. 8 plotted against areas. First, we see again $d_c < 25 \text{ km}$. Second, continent area extends up to approximately 80% of the total area of earth in the limit of three times the present crust volume. Third, ocean area correspondingly is as small as 20% in the same limit. Fourth, very small values of V_c result in vanishing continent area so that Earth is largely covered by water. Fifth, present

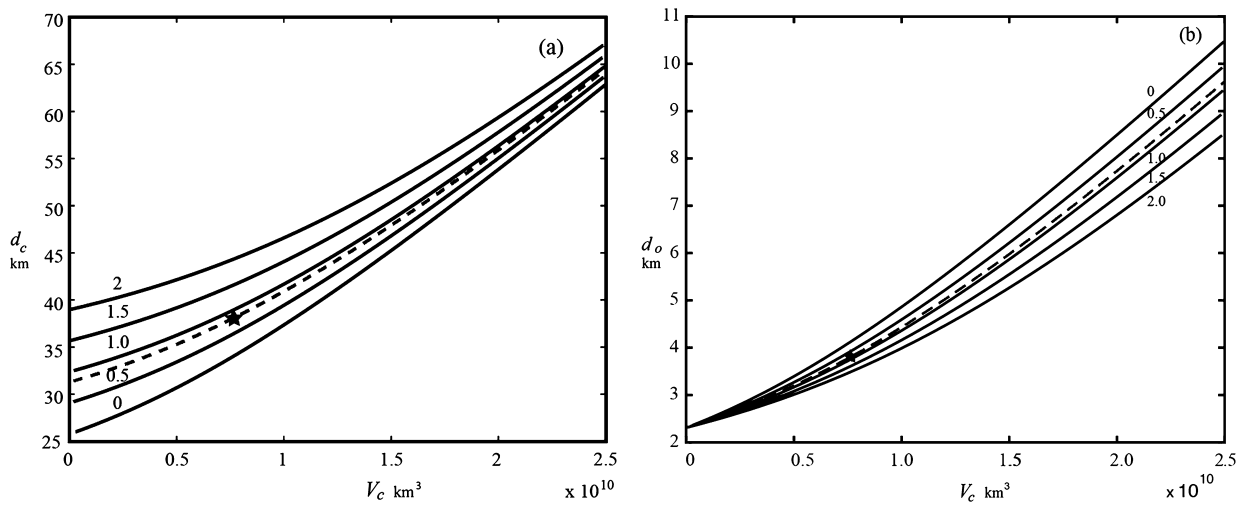


Fig. 8. (a) Thickness of the continental crust as a function of continental crust volume using (32). The solid curves are for 5 different values of mean continent elevation above sea level E (in km) and the sixth with present elevation $E = 0.835$ km is shown as a dashed curve. The star shows present Earth. (b) Ocean depth using (26). Water volume is fixed at the present value $V_o = 1.178 \times 10^9 \text{ km}^3$ and $D = -2.369$ km.

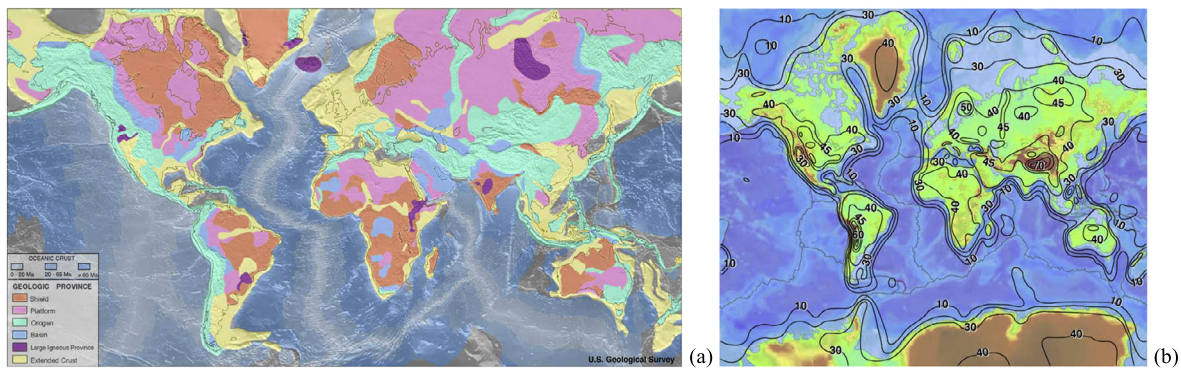


Fig. 9. (a) Map of geological provinces of the world. The shields are cratons extending to the surface and the platforms are cratons covered with sediment. (From public domain by USGS – <http://earthquake.usgs.gov/data/crust/maps.php>.) (b) Continental crust thickness (km). (From public domain by USGS – <http://quake.wr.usgs.gov/research/structure/CrustalStructure/>.)

Earth (stars) is in a region sensitive to changes so relative thickness and areas change with different volumes of materials and erosion rates. Summarizing the results shown in Figs. 8 and 10, continent crustal thickness is likely to range between the extremes of 25 to 70 km, but for all crust volumes, continent area is less than 80% of earth's area and the ocean area is more than 20%.

Next, we investigate sensitivity of continent crust thickness and ocean depth to the volume of planetary water V_o . Since past values are poorly constrained, a wide range of values of water volume from 0.01 to 10 times the present volume is used. Mean continent elevation is set to the present value $E = 0.835$ km. Fig. 11 shows crust thickness as a function of crust volume and areas. Crust thickness extends from 23.4 km to almost 180 km. Fig. 12 shows ocean depth. It ranges from almost zero to 35 km.

In summary, the analysis in this section shows that continental crust is greater than about 22 km (Figs. 8, 10, 11, and 12). With present water volume on Earth, continents occupy less than about 75% of Earth's area, and oceans occupy more than 25% of the surface area. These results assume first that there are circumstances where continents have evolved long enough for the dynamic balance described here to have become established on earth. Second, it assumes Earth has similar material properties and weathering rates so that erosion is strong enough to limit the elevation of the continent material. Third, it assumes similar values of D .

5. Summary

Floating oil thickens when subjected to convergence by an underlying fluid, but it thickens with convergence speed and thus has shortcomings as a model of continents on earth. A theoretical fluid model using an ocean layer of given thickness and Newtonian viscosity produces a tabular continent. Using the hydrostatic pressure balance under the continents and ocean basins and using the fact that the average continent surface elevation is less than 1 km above the ocean surface, calculations show that the average thicknesses and the areas of Earth's continents and oceans are readily estimated as a function of volumes of continental crust and water. For application to earlier earth, and for almost all possible volumes, the continental crust exceeds 22 km in thickness and total continent area is less than 75% of Earth's surface. This constraint may be useful to those studying the evolution of Earth. If suitable changes in surface area are made, calculations may also be useful for other earthlike planets or moons.

Admittedly, the kinetic details and consequences from erosion are crudely represented in the simplified model in section 3. This does not seem to matter because if erosion is strong enough to level mountains in a fraction of a planet's lifetime, the tabular nature of continents is not sensitive to erosion rates. Our model poorly represents other aspects of erosion, too. Material is not swept off the top of the continents, moved to the oceans or to low regions of a continent and swept into the mantle at subduc-

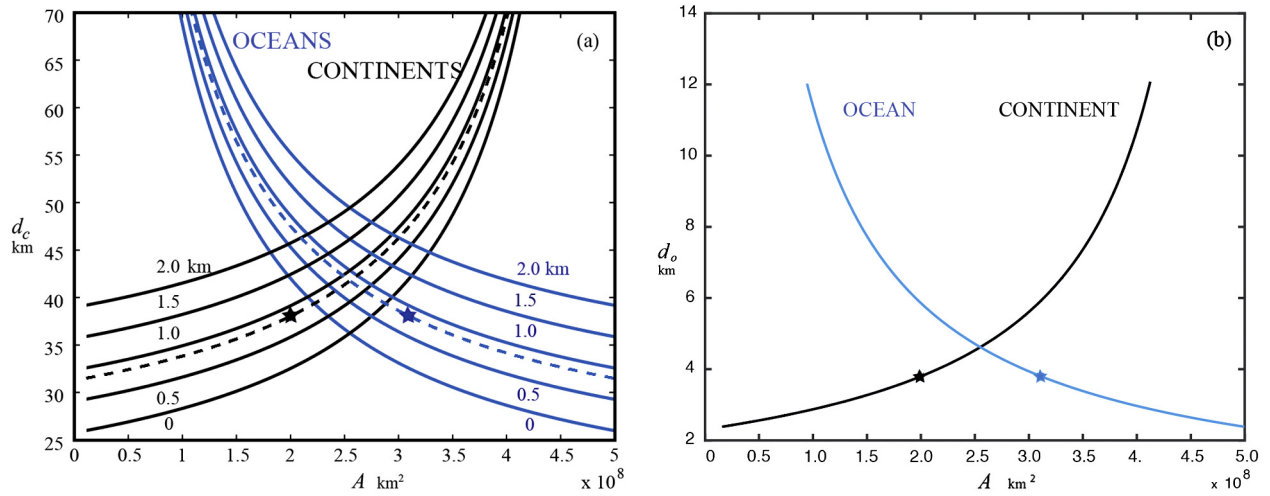


Fig. 10. (a) Continent thickness as a function of the areas of the continents and oceans. Solid curves are for 5 different values of mean continent elevation above sea level E and the sixth dashed curve is for present elevation. (b) Ocean depth versus areas of the continents and oceans collapses to a single curve for all E . Water volume is fixed at the present value $V_o = 1.178 \times 10^9 \text{ km}^3$ and $D = -2.369 \text{ km}$.

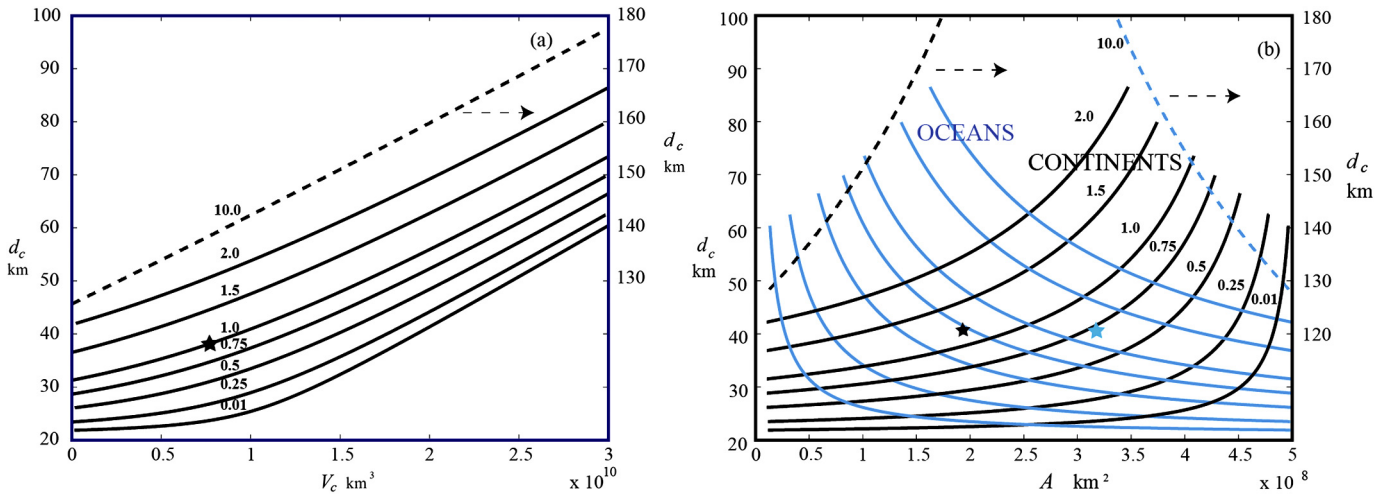


Fig. 11. Continental crust thickness for 8 values of the ratio of water volume to the present value as a function of (a) continental crust volume and (b) areas of oceans and continents (the dashed lines are offset from the solid lines and they use the scale shown on the right). The stars show present Earth. $E = 0.835 \text{ km}$ and $D = -2.369 \text{ km}$.

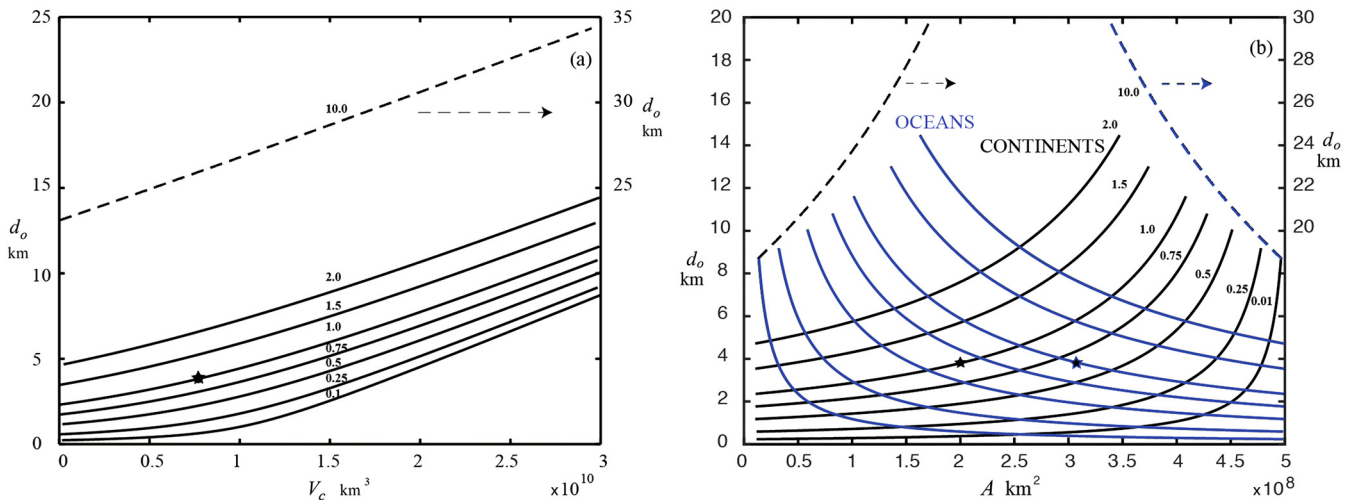


Fig. 12. As in Fig. 11 but for ocean depth instead of crust thickness.

tion zones only to be partially returned by volcanism in this model. However, even though this model does not produce a realistic cycle of mantle material from surface to mantle and back, a statement of conservation of the total continent material at any one time plus the conservation of water on the planet is used to determine areas and average thickness of oceans and continents.

The theory in Section 3 shows that tabular continents arise from the simple balance between orogeny, erosion and freeboard. This balance is likely to exist over wide ranges of governing parameters with predictable thicknesses and areas of ocean and continental crust linked to volumes of continental crust and water. In the process, water on Earth, through the act of erosion on land (and water on any other earthlike planet), has carved its own cistern. This cistern, the ocean, holds most all of the water and causes orogeny and erosion on the continents to form tabular continents. Note also that the tabular nature of continents certainly has effects on the collision and breaking apart of the individual continents during Wilson cycles. Therefore, Earth's water exerts a first order effect on the areas of continents and oceans and presumably thereby it affects the pattern of mantle circulation throughout all the depth of the mantle possibly all the way to the core.

Acknowledgements

Conversations with many of the participants of the Woods Hole Oceanographic Geodynamics program stimulated this study. I particularly thank Stan Hart, Peter Molnar, and Peter Clift for useful suggestions over the course of the work.

Appendix A. The deflection of a crustal layer by mantle circulation

This two-layer calculation gives the amount of thickening and thinning of floating fluid from circulation of fluid below in the limit of large viscosity (Whitehead, 2003). A layer of viscous fluid representing continental crust lies above a circulating mantle. The top layer (Fig. A.1) has viscosity, μ_1 density ρ_1 and average thickness d . It lies above the "mantle" fluid with viscosity μ_2 density ρ_2 , and average depth D_m in a field of gravity g . Simplifications are: 1. Only steady flows are considered. 2. The matching conditions between layers are applied at the level mean interfaces so that the equations are linear. 3. The flows exist for small Reynolds number so that inertial forces are much smaller than viscous forces. 4. The flow is two-dimensional.

Accordingly, the equations of two-dimensional viscous flow are used

$$0 = -\nabla p_i + \mu_i \nabla^2 \tilde{u}_i \quad (\text{A.1})$$

where $i = 1, 2$ denote the top and bottom layers, respectively, with $\tilde{u}_i = u_i \hat{i} + w_i \hat{j}$ and the \hat{i} and \hat{j} unit vectors in the horizontal and vertical directions. The continuity equation is

$$\frac{\partial u_i}{\partial x} + \frac{\partial w_i}{\partial z} = 0. \quad (\text{A.2})$$

The boundary conditions at the interface between the two layers (which is taken to be at $z = 0$) are the matching of lateral velocity $u_1 = u_2$ vertical velocity $w_1 = w_2$, and lateral stress

$$\mu_1 \left(\frac{\partial u_1}{\partial z} + \frac{\partial w_1}{\partial x} \right) = \mu_2 \left(\frac{\partial u_2}{\partial z} + \frac{\partial w_2}{\partial x} \right).$$

In addition, the condition of vertical stress determines a value for interface deflection η_2 .

$$2\mu_1 \frac{\partial u_1}{\partial x} + P_1 - 2\mu_2 \frac{\partial u_2}{\partial x} - P_2 = g(\rho_2 - \rho_1)\eta_2 \quad (\text{A.3})$$

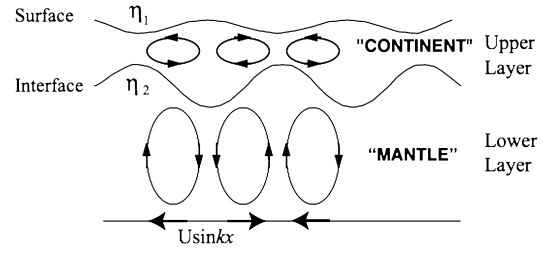


Fig. A.1. The two layer model driven by velocity at the lower boundary.

Boundary conditions on the top of the upper layer are applied at $z = d$. These conditions are zero vertical velocity, zero lateral stress (often called free-slip), and zero vertical stress that will produce a value for η_1 . The final two boundary conditions are imposed at the bottom of the deep layer at $z = -D_m$. They are that the vertical velocity is equal to zero, that $w_2 = 0$, and that the imposed velocity $u_2 = U \sin kx$.

The solutions are of the form

$$w_i = \{A_i \sinh kz + B_i z \sinh kz + C_i z \cosh kz\} \cos kx. \quad (\text{A.4})$$

The boundary and interface conditions can be expressed as the matrix equation

$$\begin{vmatrix} kcD & -sD - kD_m cD & cD + kD_m sD & 0 & 0 & 0 \\ -sD_m & D_m sD & -D_m cD & 0 & 0 & 0 \\ k & 0 & 1 & -k & 0 & -1 \\ 0 & \mu_2 & 0 & 0 & -\mu_1 & 0 \\ 0 & 0 & 0 & sd & dsd & dcd \\ 0 & 0 & 0 & 2k^2 sd & 2kcd + 2k^2 dsd & 2ksd + 2k^2 dcd \end{vmatrix}$$

$$\times \begin{vmatrix} A_2 \\ B_2 \\ C_2 \\ A_1 \\ B_1 \\ C_1 \end{vmatrix} = \begin{vmatrix} Uk \\ 0 \\ 0 \\ 0 \\ 0 \\ 0 \end{vmatrix} \quad (\text{A.5})$$

where $cD = \cosh kD_m$, $cd = \cosh kd$, $sD = \sinh kD_m$ and $sd = \sinh kd$. The solutions for the constants are

$$A_1 = 2Uk^2 \mu_2 [sD - kD_m cd] / \text{Det}$$

$$B_1 = 2Uk^2 \mu_2 [sD - kD_m cD] (sd)^2 / \text{Det}$$

$$C_1 = -2Uk^2 \mu_2 [sD - kD_m cd] sdcd / \text{Det}$$

$$A_2 = 2Uk^2 [\mu_1 D_m sD (sd)^2 + \mu_2 D_m cD (-kd + sdcd)] / \text{Det}$$

$$B_2 = 2Uk^2 [\mu_1 (sD - kD_m cD) (sd)^2] / \text{Det}$$

$$C_2 = 2Uk^2 [-\mu_1 kD_m sD (sd)^2 + \mu_2 sD (kd - sdcd)] / \text{Det}$$

where

$$\text{Det} = -2k\mu_1 [(sD)^2 - k^2 D_m^2] (sd)^2 + 2k\mu_2 [sDcD - kD_m] [kd - sdcd].$$

The solution for η_1 gives values of the elevation of the surface corresponding to continent elevation

$$\frac{\eta_1}{d} = \eta_{01} \times \frac{[kD_m \cosh kD_m - \sinh kD_m] [2kd \cosh kd - 3 \sinh kd]}{[\sinh^2 kD_m - k^2 D_m^2] \sinh^2 kd + \mu_0 [\sinh kD_m \cosh kD_m - kD_m] [\sinh kd \cosh kd - kd]} \quad (\text{A.6})$$

where $\eta_{01} = \frac{2Uk^2 \mu_2}{g\rho_1}$ and $\mu_0 = \mu_2 / \mu_1$. The solution for η_2 gives the depth of the deflection of the interface between the two fluids corresponding to "continental roots"

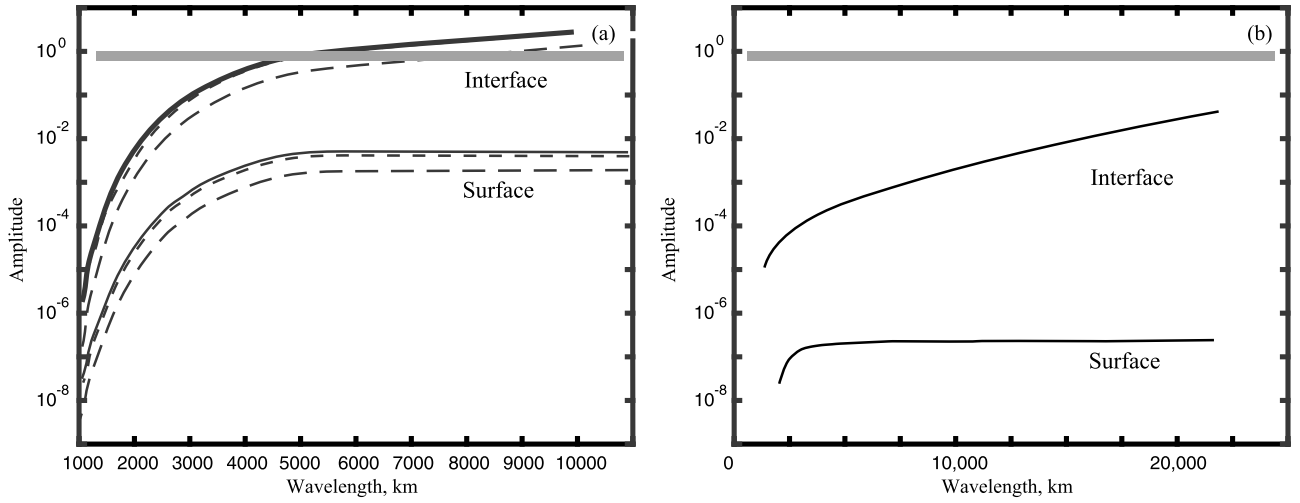


Fig. A.2. Elevation of the surface of the top layer and the interface between the two layers as a function of the driving wavelength. (a) Results for a deep mantle flow. The long dashed lines are for $\mu_0 = 10^2$ the short dashed lines are for $\mu_0 = 10^{-2}$ and the solid lines are for equations (A.1) and (A.2). The thick gray line indicates the order one amplitude limit of the calculation. (b) Results for shallow lower layer. The symbols are from the approximations in equations (A.1) and (A.2) and the solid curves from equations (A.6) and (A.7).

$$\frac{\eta_2}{d} = \eta_{02} \times \frac{[kD_m \cosh kD_m - \sinh kD_m] + \lambda \sinh kD_m \sinh^2 kd + \mu_0 \lambda \cosh kD_m [\sinh kd \cosh kd - kd]}{[\sinh^2 kD_m - k^2 D_m^2] \sinh^2 kd + \mu_0 [\sinh kD_m \cosh kD_m - kD_m] [\sinh kd \cosh kd - kd]} \quad (\text{A.7})$$

where $\eta_{02} = \frac{2Uk^2\mu_2}{g(\rho_2 - \rho_1)}$ and $\lambda = D_m/d$.

Since continental crust is very thin compared to the depth of the mantle we take kd small in (A.6) and (A.7) and also take the crust to be more viscous than the mantle (England and Molnar, 1997), so $\mu_0 = \mu_2/\mu_1 \ll 1$. Then, (A.6), (A.7) simplify to

$$\frac{\eta_1}{d} = \frac{-2U\mu_2k[kD_m \cosh kD_m - \sinh kD_m]}{g\rho_1d[\sinh^2 kD_m - k^2 D_m^2]} \quad (\text{A.8})$$

$$\eta_2 = \frac{-\rho_1\eta_1}{\rho_2 - \rho_1} \quad (\text{A.9})$$

An important result in these limits is that the viscosity of the top layer has dropped out and is not important in determining the deflections. This arises because the surface and the interface develop values that allow stress from the mantle circulation to balance buoyant restoring forces produced by topography. Therefore, this simplified model of the production of continent by mantle convergence does not depend on the viscosity of the continents, or if continent viscosity is a proxy for a very small value of erosion, it does not depend on the strength of erosion.

Fig. A.2 shows values of deflection divided by layer depth for equations (A.6) and (A.7) and for equations (A.8) and (A.9). For this calculation, the velocity $U = 3 \times 10^{-9} \text{ m s}^{-1}$ was used, which is the spreading rate of the Pacific plate. This model therefore has the same magnitude for the flow speeds in the deep and top shallow mantle, which is appropriate for uniform viscosity mantle convection. The other parameters used are the acceleration of gravity $g = 9.8 \text{ m s}^{-2}$, density difference between mantle and continent with the typical value $\rho_2 - \rho_1 = 600 \text{ kg/m}^3$, and upper layer thickness $d = 15 \text{ km}$. This is the value if all continental crust were spread evenly over the globe. This calculation is an estimate of what happens in two cases, first, before the continent material is segregated into lumps and second, what happens in the experiments in Fig. 2. Panel (a) has the results for whole mantle convection with $D_m = 2880 \text{ km}$. The viscosity used is the well-known value for deep mantle convection 10^{21} Pa s . The ratio of viscosity between the lower and upper layer are $\mu_0 = 0.01$ and 100 in

equations (A.6) for the surface and (A.7) for the interface (long and short dashes, respectively). In addition, curves from equations (A.8) and (A.9) are plotted as solid curve and they lie very close to the curve for $\mu_0 = 0.01$, so that excellent agreement exists between the general formulas and the approximations. Generally speaking, the value of the viscosity of the upper layer is not important as long as viscosity is more than ten times greater than mantle viscosity.

For parameters with the deflection of order one, the layer would break up and the calculation is invalid. Panel (a) indicates that cells with wavelength greater than about 6000 km produce interface deflections indicating break up (thick gray line). Therefore, in this model, continental crust could not cover earth but would instead be broken up into lumps of individual continent. Panel (a) also shows that wavelengths shorter than about 5000 km would not form proto-continent, but longer wavelengths produce a bottom interface amplitude of order one.

The size of deflection for parameters associated with shallow mantle convection (mantle layer 600 km deep and viscosity of 10^{19} Pa s) are shown in Fig. A.2b. The break-up criterion is not found since the amplitude is not close to one even for the longest wavelength mantle motion.

A close view of the velocity field using parameters for both the crust and mantle with $\mu_0 = 10$ is shown in Fig. A.3. The upper panel has stretched vertical coordinates and a different velocity axis scale than the lower panel. The predominant stress exerted by the lower layer onto the upper layer is from shear $\mu_2[\frac{\partial w_2}{\partial z}]$ (the boundary condition $w = 0$ imposes the stress component $\mu_2[\frac{\partial w_2}{\partial x}] = 0$). The shear imposed by the lower layer drives a flow in the upper layer that has a return flow near the surface driven by the surface elevation slope. The overturning cell in the top layer is opposite in sense from the overturning cell in the lower layer. The shear exerted by the bottom circulation is almost completely balanced by the surface elevation slope so that the surface elevation slope is not a function of the viscosity of the upper layer. The balance between surface elevation and stress at the base of the surface layer might also be true for mountain belts over a convecting mantle and thus used to estimate shear stress that the mantle exerts on the bottom of mountain belt. The stress induced by surface slope has been used in conjunction with Global positioning data of divergence to estimate an equivalent viscosity for the Himalayas (England and Molnar, 1997).

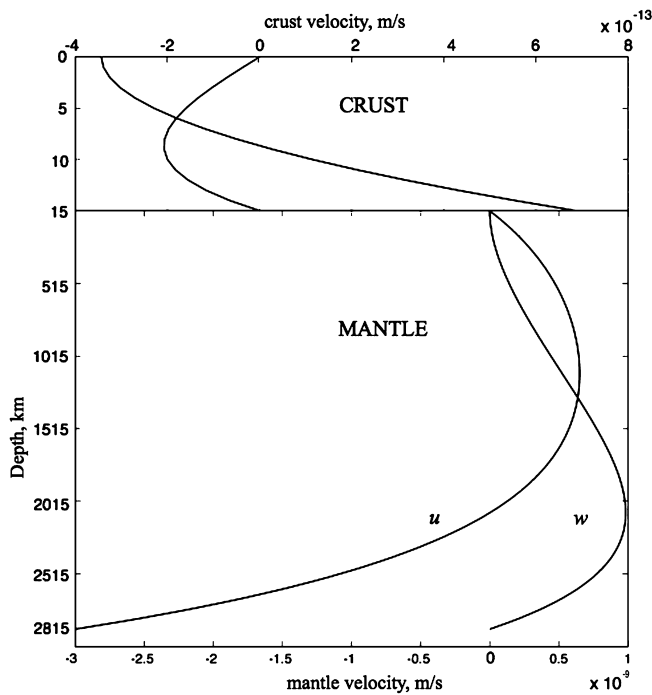


Fig. A.3. Lateral and vertical velocity profiles.

Finally this is applied to the roller experiment shown in Fig. 3 using (A.8) and (A.9) and simplifying near the origin

$$\eta_1 = \frac{3U\mu}{2\rho_1 g D_m} \quad (\text{A.10})$$

and for the surface between oil and syrup

$$\eta_2 = \frac{3U\mu}{2(\rho_2 - \rho_1)gd^2k}. \quad (\text{A.11})$$

We use velocity given by $U = 2\pi\Omega$, and the following physical values: syrup density $\rho_2 = 1439 \text{ kg/m}^3$, silicon oil density $\rho_1 = 1020 \text{ kg/m}^3$, syrup viscosity 32.3 Pas , with roller radius $r = 0.018 \text{ m}$, depth between rollers and the oil/syrup interface $d = 0.04 \text{ m}$, and wavenumber $k = 39 \text{ m}^{-1}$ to get, in meters,

$$\eta_1 = 1.36 \times 10^{-3} \Omega \quad (\text{A.12})$$

and

$$\eta_2 = 3.31 \times 10^{-3} \Omega. \quad (\text{A.13})$$

These are shown as dashed curves in Fig. 3.

Appendix B. Supplementary material

Supplementary material related to this article can be found online at <http://dx.doi.org/10.1016/j.epsl.2017.03.017>.

References

Bird, P., 1979. Continental delamination and the Colorado Plateau. *J. Geophys. Res.* 84 (B13), 7561–7571.

Clift, P.D., Vannuchi, P., 2004. Controls on tectonic accretion versus erosion in subduction zones: implications for the origin and recycling of the continental crust. *Rev. Geophys.* 42, RG2001. <http://dx.doi.org/10.1029/2003RG000127>.

Clift, P.D., Vannucchi, P., Morgan, J.P., 2009. Crustal redistribution, crust–mantle recycling and Phanerozoic evolution of the continental crust. *Earth-Sci. Rev.* 97 (1), 80–104.

Cogley, J.G., 1984. Continental margins and the extent and number of continents. *Rev. Geophys.* 22 (2), 101–122. <http://dx.doi.org/10.1029/RG022i002p0101>.

Condie, Kent C., 2016. *The Earth as an Evolving Planetary System*. Academic Press, Elsevier.

Conrad, C.P., Molnar, P., 1997. The growth of Rayleigh–Taylor-type instabilities in the lithosphere for various rheological and density structures. *Geophys. J. Int.* 129, 95–112.

Dewey, J.F., Windley, B.F., 1981. Growth and differentiation of the continental crust. *Philos. Trans. R. Soc. Math. Phys. Eng. Sci.* 301, 189–206.

England, P., Molnar, P., 1997. Active deformation of Asia: from kinematics to dynamics. *Science* 278 (5338), 647–650.

Eriksson, P.G., 1999. Sea level changes and the continental freeboard concept: general principles and application to the Precambrian. *Precambrian Res.* 97 (30), 143–154.

Flesch, L.M., Holt, W.E., Haines, A.J., Shen-Tu, B., 2000. Dynamics of the Pacific–North American plate boundary in the Western United States. *Science* 287, 834–836.

Gazel, E., Hayes, J.L., Hoernle, K., Kelemen, P., Everson, E., Holbrook, W.S., Yogodzinski, G.M., 2015. Generation of continental crust in oceanic arcs. *Nat. Geosci.* 8, 321–327.

Gossler, J., Kind, R., 1996. Seismic evidence for very deep roots of continents. *Earth Planet. Sci. Lett.* 138, 1–13.

Grotzinger, J., Jordan, T.H., 2010. *Understanding Earth*. Macmillan.

Harrison, C.G.A., 1988. Eustasy and epeirogeny of continents on time scales between about 1 and 100 m.y. *Paleoceanography* 3, 671–684.

Harrison, C.G.A., 1990. Longterm eustasy and epeirogeny in continents. In: *Sea-Level Change*. Nat. Acad. Press, Washington, DC, pp. 141–158.

Harrison, C.G.A., 1994. Rates of continental erosion and mountain building. *Int. J. Earth Sci.* 83, 431–447.

Harrison, C.G.A., 1998. The hypsography of the ocean floor. *Phys. Chem. Earth* 23, 761–774.

Harrison, C.G.A., 1999. Constraints of ocean volume change since the Archean. *Geophys. Res. Lett.* 26, 1913–1916.

Harrison, C.G.A., Brass, G.W., Saltzman, E., Sloan II, J., Southam, J., Whitman, J.M., 1981. Sea level variations, global sedimentation rates and the hypsographic curve. *Earth Planet. Sci. Lett.* 54, 1–16.

Harrison, C.G.A., Miskell, K.J., Brass, G.W., Saltzman, E.S., Sloan II, J., 1983. Continental hypsography. *Tectonics* 2, 357–377.

Harrison, C.G.A., Brass, G.W., Miskell-Garhardt, K., Saltzman, E., 1985. Reply. *Tectonics* 4, 257–262.

Hawkesworth, C.J., Dhuime, B., Pietranik, A.B., Cawood, P.A., Kemp, A.I.S., Storey, C.D., 2010. The generation and evolution of the continental crust. *J. Geol. Soc.* 167, 229–248. <http://dx.doi.org/10.1144/0016-76492009-072>.

Höning, D., Spohn, T., 2016. Continental growth and mantle hydration as intertwined feedback cycles in the thermal evolution of Earth. *Phys. Earth Planet. Inter.* 255, 27–49.

Houseman, G.A., Molnar, P., 1997. Gravitational (Rayleigh–Taylor) instability of a layer with non-linear viscosity and convective thinning of continental lithosphere. *Geophys. J. Int.* 128, 125–150.

Huerta, A., Royden, L., Hodges, K., 1996. The interdependence of deformational and thermal processes in mountain belts. *Science* 273, 637–639.

Huerta, A., Royden, L., Hodges, K., 1998. The thermal structure of collisional orogens as a response to accretion, erosion, and radiogenic heating. *J. Geophys. Res.* 103 (B7), 15,287–15,302.

Huerta, A., Royden, L., Hodges, K., 1999. The effects of accretion and erosion on the metamorphic evolution of collisional orogens. *J. Metamorph. Geol.* 17, 349–366.

Hynes, A., 2001. Freeboard revisited: continental growth, crustal thickness change and Earth's thermal efficiency. *Earth Planet. Sci. Lett.* 185, 161–172.

Johnson, Michael R.W., Harley, Simon L., 2012. *Orogenesis: The Making of Mountains*. Cambridge University Press.

Kaufman, P.S., Royden, L.H., 1994. Lower crustal flow in an extensional setting: constraints from the Halloran Hills region, Eastern Mojave Desert, California. *J. Geophys. Res.* 99, 15723–15739.

Kay, R.W., Kay, S.M., 1993. Delamination and delamination magmatism. *Tectonophysics* 219, 177–189.

Kearey, P., Klepeis, K.A., Vine, F.J., 2009. *Orogenic belts*. In: *Global Tectonics*, 3rd ed. Wiley–Blackwell. ISBN 1-4051-0777-4, p. 287 (Chapter 10).

King, Scott D., 2005. Archean cratons and mantle dynamics. *Earth Planet. Sci. Lett.* 234 (1), 1–14.

King, Scott D., 2015. Mantle convection, the asthenosphere, and Earth's thermal history. *Spec. Pap., Geol. Soc. Am.* 514, 87–103.

Kuhn, William R., Walker, J.C.G., Marshall, Hal G., 1989. The effect on Earth's surface temperature from variations in rotation rate, continent formation, solar luminosity, and carbon dioxide. *J. Geophys. Res., Atmos.* 94 (D8), 11129–11136.

McElroy, B., Wilkinson, B., 2005. Climatic control of continental physiography. *J. Geol.* 113 (1), 47–58.

McLennan, S.M., Taylor, S.R., 1983. Continental freeboard, sedimentation rates and growth of continental crust. *Nature* 306, 169–172. <http://dx.doi.org/10.1038/306169a0>.

Müller, R.D., Sdrolias, M., Gaina, C., Steinberger, B., Heine, C., 2008. Long-term sea-level fluctuations driven by ocean basin dynamics. *Science* 319, 1357–1362. <http://dx.doi.org/10.1126/science.1151540>.

O'Neill, C., Lenardic, A., Condie, K.C., 2015. Earth's punctuated tectonic evolution: cause and effect. *Geol. Soc. (Lond.) Spec. Publ.* 389 (1), 17–40.

Press, F., 2003. *Understanding Earth*, 4th ed. Macmillan. ISBN 0-7167-9617-1, pp. 468–469.

- Roberts, N.M.W., van Kranendonk, M.J., Parman, S., Shirey, S., Clift, P.D. (Eds.), 2015. *Continent Formation Through Time*. Geol. Soc. (Lond.) Spec. Publ., vol. 389. 362 pp.
- Royden, L., 1993a. The evolution of retreating subduction boundaries formed during continental collision. *Tectonics* 12, 629–638.
- Royden, L., 1993b. The tectonic expression of slab pull at continental convergent boundaries. *Tectonics* 12, 303–325.
- Saal, A.L., Rudnick, R.L., Ravizza, G.E., Hart, S.R., 1998. Re–Os isotope evidence for the composition, formation and age of the lower continental crust. *Nature* 393 (6680), 58–61. <http://dx.doi.org/10.1038/29966>.
- Schubert, G., Reymer, A.P.S., 1985. Continental volume and freeboard through geological time. *Nature* 316, 336–339.
- Schubert, G., Sandwell, D., 1989. Crustal volumes of the continents and of oceanic and continental submarine plateaus. *Earth Planet. Sci. Lett.* 92 (2), 234–246.
- Sverdrup, H.U., Johnson, M.W., Fleming, R.H., 1942. *The Oceans: Their Physics, Chemistry, and General Biology*, vol. 7. Prentice-Hall, New York.
- Taylor, S.R., McLennan, S.M., 1995. The geochemical evolution of the continental crust. *Rev. Geophys.* 33, 241–265. <http://dx.doi.org/10.1029/95RG00262>.
- Thatcher, W., Foulger, G.R., Julian, B.R., Svarc, J., Quilty, E., Bawden, G.W., 1999. Present-day deformation across the Basin and Range Province, Western United States. *Science* 283, 1714–1718.
- Turcotte, D.L., Schubert, G., 2002. *Geodynamics*. Cambridge University Press, New York. 456 pp.
- Uchupi, Elazar, Emery, Kenneth O., 1993. *Morphology of the Rocky Members of the Solar System*. Springer Science & Business Media. 394 pp.
- Veizer, J., Jansen, S.L., 1985. Basement and sedimentary recycling – 2: time dimension to global tectonics. *J. Geol.* 93, 625–643.
- Walther, John Victor, 2005. *Essentials of Geochemistry*. Jones & Bartlett. ISBN 0-7637-2642-7, p. 35.
- Whitehead, J.A., 2003. Laboratory studies of mantle convection with continents and other GFD problems. In: *Recent Research Developments in Fluid Dynamics*. Transworld Research Network, Kerala, India.
- Whitehead, J.A., Clift, P.D., 2009. Continent elevation, mountains, erosion – freeboard implications. *J. Geophys. Res. B* 114, B05410. <http://dx.doi.org/10.1029/2008JB006176>.
- Wise, Donald U., 1972. Freeboard of continents through time. *Geol. Soc. Am. Mem.* 132, 87–100.
- Wise, Donald U., 1974. Continental margins, freeboard and the volumes of continents and oceans through time. In: *The Geology of Continental Margins*. Springer, Berlin, Heidelberg, pp. 45–58.
- Yin, A., Harrison, T.M., 2000. Geologic evolution of the Himalayan–Tibetan orogens. *Annu. Rev. Earth Planet. Sci.* 28, 211–280.
- Zhang, Youxue, 2005. Global tectonic and climatic control of mean elevation of continents, and Phanerozoic sea level change. *Earth Planet. Sci. Lett.* 237, 524–531.